Energy Proceedings
Vol 41, 2024
ISSN 2004-2965

Thermodynamic Analysis of Cerium-Based Solar Thermochemical Cycle for Carbon Monoxide Production

Yibiao Long[1,2], Fan Jiao[1], Shiying Yang[1,2], Taixiu Liu[1], Qibin Liu[1,2*]

1 Institute of Engineering Thermophysics, Chinese Academy of Science, Beijing 100190, China

2 University of Chinese Academy of Science, Beijing, 100190, China

(*Corresponding Author: qibinliu@iet.cn)

ABSTRACT

Solar thermochemical decomposition of CO_2 for fuel production is a promising pathway to achieve efficient and stable solar energy applications. Among these methods, Ce-based two-step thermochemical cycles have received increasing attention. To date, a comprehensive thermodynamic assessment of such thermochemical cycle is still lacking, especially in terms of exergy. In this study, a new exergy analysis model for the solar Ce-based thermochemical cycle is developed, with the aim of exploring the potential to improve efficiency according to irreversibility distribution. Through a careful study of the relation between the three independent variables (reduction temperature T_H, Oxidation temperature T_L, and pressure P) and efficiency, we put forth new strategies to reduce various energy and exergy losses. Based on the permutation algorithm, we find the operating conditions with the lowest irreversibility, which results in a 141% improvement in energy efficiency and a 91% improvement in exergy efficiency compared to the highest efficiency case.

Keywords: Solar energy, Thermochemical cycles, Fuel production, Exergy analysis

NONMENCLATURE

Abbreviations	
STF	Solar To Fuel
IRR	Irreversibility
EXC	Heat Exchanger

Symbols	
I	Direct Normal Irradiance, 1000W/m^2
C	Concentration Ratio, 3000 suns
δ	Stoichiometric number
n	Amount of Substance, mol
T_H	Temperature at Reduction Reactor, K
T_L	Temperature at Oxidation Reactor, K
T_0	Surrounding Temperature, 298K
P_{O_2}	Partial Pressure of Oxygen, bar
σ	Boltzmann constant, 5.67x10^{-8}W/(m^{2}K^4)
$Q_{re,reactor}$	Net Heat Absorbed at Reduction Reactor
$Q_{re,radloss.reducer}$	Heat Loss of Reduction Reactor via Re-radiation
$Q_{cooler1}$	Heat Loss of Cooler-1
$Q_{oxi,reactor}$	Heat Loss of Oxidation Reactor
Q_{EXC}	Heat Loss of Heat Exchanger
$Q_{re,reactor}^{solar}$	Solar Radiation Received at Reduction Reactor from sun
$W_{pump,fact}$	Work Needed to Operate Vacuum Pump
$\eta_{abs,reduction}$	Absorption Rate of Reduction Reactor

This is a paper for 15th International Conference on Applied Energy (ICAE2023), Dec. 3-7, 2023, Doha, Qatar.

η_{STF}	Solar-to-Fuel Energy Efficiency
$IRR_{re,reactor}$	Irreversibility of Reduction Reactor
$IRR_{oxi,reactor}$	Irreversibility of Oxidation Reactor
$IRR_{cooler1}$	Irreversibility of Cooler-1
$IRR_{cooler2}$	Irreversibility of Cooler-2
IRR_{EXC}	Irreversibility of Heat Exchanger

1. INTRODUCTION

The use of solar energy for energy supply is one of the sustainable ways to alleviate current energy and environmental issues[1,2]. Solar thermochemical CO_2 splitting for fuel production is considered to be an ideal method, due to the advantages of resource utilization of CO_2 and storing unstable solar energy as a stable fuel chemical energy[3]. Among numerous technology routes, the solar Ce-based thermochemical cycle for decomposing CO_2 (see Eqs.(1) and (2)) receives increasing attention due to its lower temperature for fuel production and the automatic separation of O_2 and CO products as compared with direct CO_2 decomposition methods.

Reduction Reaction: $\frac{1}{\delta}CeO_2 = \frac{1}{\delta}CeO_{2-\delta} + \frac{1}{2}O_2$

Oxidation Reaction: $\frac{1}{\delta}CeO_{2-\delta} + CO_2 = \frac{1}{\delta}CeO_2 + CO$

Total Reaction: $CO_2 = CO + \frac{1}{2}O_2$

The efficiency analysis has been intensively studied. Abanades et al[4] conducted an energy analysis of the CeO_2/Ce_2O_3 solar thermochemical cycle and obtained a theoretical maximum cycle efficiency. However, this cycle did not attract wide attention due to the poor stability under the high operating temperature over 2273 K. William et al[5] performed thermodynamic analyses on Ce-based solar thermochemical cycles that involve reactions with non-stoichiometric coefficients. It reaches 16-19% solar-to-fuel conversion efficiency without heat recovery at a relatively mild temperature. Then non-stoichiometric Ce-based thermochemical cycle become a popular research topic. Similarly, Zhu et al[6] conducted thermodynamic analyses of this cycle with various proportions of Zr doping in CeO_2. In experiments, Zr-doped ceria shows the highest productivity. Previous studies focused only on energy analysis, without exergy analysis, leading to the absence of understanding of the irreversibility in this typical solar thermochemical cycle.

In this study, the thermodynamic analysis of the solar Ce-based thermochemical cycle for CO production is conducted by a general energy and irreversibility model. Under experimental operation conditions[7], which is the highest experimental STF efficiency, the distribution of energy and exergy loss is studied to find out the potential to improve efficiency. Based on the model, we elucidate the relations between the three characteristic variables (T_H, T_L, and P) and different forms of losses. Through the permutation algorithm, we find the working condition with the lowest irreversibility and give suggestions to subsequent experiments.

2. THERMODYNAMIC MODEL

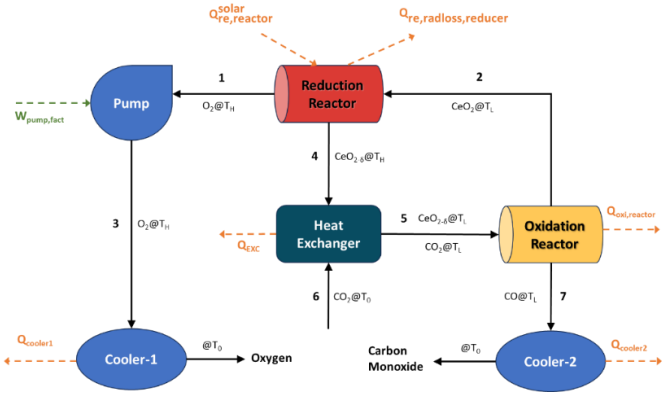

Fig. 1 Flowsheet of Ce-based thermochemical cycle

The flow sheet of the solar Ce-based thermochemical cycle from an existing experimental study is shown in Fig. 1. It comprises the endothermic and reduction reaction processes, heat exchange process, exothermic and oxidation reaction process of the solar thermochemical cycle, which occurs in the reduction reactor, heat exchanger, and oxidation reactor, respectively. To maintain a low oxygen partial pressure in the reduction reactor, Ar is used for purging, gas are pumped out through a vacuum pump and discharged into the environment after cooling through Cooler-1. The CO produced is cooled down by Cooler-2 and vented to the environment. CO_2 at room temperature is preheated by the heat exchanger and enters the oxidation reactor.

The thermodynamic calculations in this study will be based on the following assumptions: only the reradiation losses from the reduction reactor are considered, not piping losses; no chemical reactions occur within the heat exchanger; calculatios are based on 1 mol produced CO.

The value of δ is calculated using the method proposed by Bulfin et al [8]:

$$\left(\frac{\delta}{\delta_m-\delta}\right)^n=\left(\frac{P_{O_2}}{P^0}\right)^{-0.5}\exp\left(\frac{\Delta s_{th}}{R}\right)\exp\left(\frac{-\Delta h_\delta^0}{RT}\right) \quad (1)$$

where $\Delta h_\delta^0=395-31.4\,log(\delta)\ kJ\cdot mol^{-1}$, $n=\frac{1}{\delta_m}=2.9$,and $\Delta s_{th}=165\,J\cdot K^{-1}mol^{-1}$.

The efficiency of the vacuum pump is computed according to the method outlined by Brendelberger et al [9]:

$$\eta_{pump}=A_0+A_1\lg\left(\frac{p_{in}}{p_{atm}}\right)+A_2\left[\lg\left(\frac{p_{in}}{p_{atm}}\right)\right]^2+A_3\left[\lg\left(\frac{p_{in}}{p_{atm}}\right)\right]^3+A_4\left[\lg\left(\frac{p_{in}}{p_{atm}}\right)\right]^4 \quad (2)$$

where $A_0=0.30557$, $A_1=-0.17808$, $A_2=-0.15514$, $A_3=-0.03173$, and $A_4=-0.00203$.

In terms of energy analysis, the heat loss is given by:

$$Q_i=\sum_j n_j\Delta H_j+\Delta H_{reaction} \quad (3)$$

where $\sum_j n_j\Delta H_j$ stands for reactants and enthalpy change of gas; $\Delta H_{reaction}$ stands for enthalpy change caused by chemical reaction; Q_i stands for the heat loss of oxidation reactor. It also stands for the heat loss of Cooler-1, Cooler-2 and heat exchanger without $\Delta H_{reaction}$ in the equation.

The equation of heat loss through re-radiation in a reduction reactor is as follows:

$$Q_{re,radloss.reducer}=\frac{Q_{re,reactor}}{\eta_{abs,reduction}}-Q_{re,reactor} \quad (4)$$

where $\eta_{abs,reduction}$ is the absorption rate of reduction reactor and it equals to $1-\frac{\sigma T_H^4}{IC}$; $\frac{Q_{re,reactor}}{\eta_{abs,reduction}}$ denoted by $Q_{re,reactor}^{solar}$, is the solar radiation received at reduction reactor from sun.

The equation of solar-to-fuel energy efficiency is shown below:

$$\eta_{STF}=\frac{HHV_{CO}}{Q_{re,reactor}^{solar}+W_{pump,fact}} \quad (5)$$

where HHV_{CO} is the high heat value of CO.

In terms of exergy analysis, the equation of irreversible loss caused by heat transfer is shown below:

$$IRR_{heat\ transfer}=\pm\frac{\Delta H_{heat}}{T}+\sum_j n_j\Delta S_j \quad (6)$$

where $\pm\frac{\Delta H_{heat}}{T}$ is the entropy flow happened at heat absorber (positive) or releaser (negative); $\sum_j n_j\Delta S_j$is the total entropy change of the reactants or gas in each unit.

The equation of irreversibility of chemical reaction is shown as follows:

$$IRR_{reaction}=-\sum_j\frac{n_j\Delta G_j}{T_j} \quad (7)$$

The total irreversibility is computed by:

$$IRR_i=IRR_{heat\ transfer}+IRR_{reaction} \quad (8)$$

where IRR_i stands for the irreversibility of Oxidation Reactor, Heat Exchanger, Cooler-1 and Cooler-2. The irreversibility of the reduction reactor should include the irreversibility caused by reradiation, as shown below:

$$IRR_{reradiation}=\frac{Q_{re,radloss,reducer}}{T_0} \quad (9)$$

Based on the definition of the solar-to-fuel energy efficiency and heat loss, we validated the model by incorporating experimental conditions into the model, and the results are shown in Fig. 2. The STF efficiency calculated by the model is 5.94%, which is closely aligned with the actual observation value (5.25%). As a result, the model is validated.

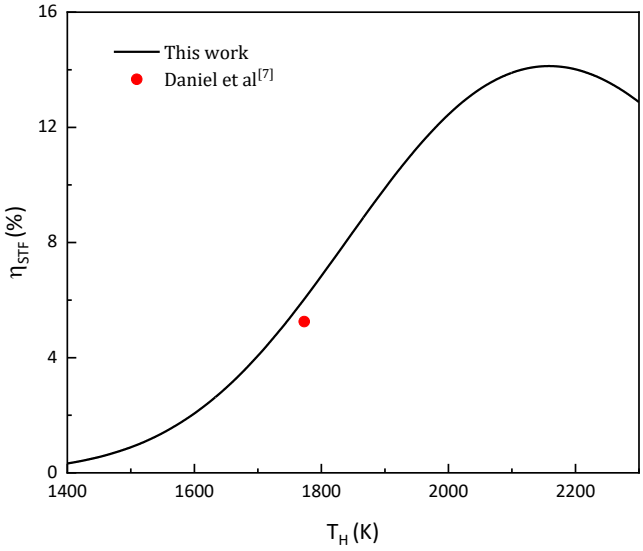

Fig. 2 η_{STF} Comparation between calculation result and experiment result from Daniel et al[7].

3. RESULTS

3.1 Overall distribution of energy losses and irreversibility

Fig. 3 shows the distribution of energy loss in the solar Ce-based thermochemical cycle at reduction and oxidation temperatures of 1773 K and 1148 K, respectively, and a pressure of 10^{-2} bar.

It is found that the energy losses from heat rejection in the heat exchanger (Q_{EXC}) are the largest, which accounts for 70.3% of the solar energy input. The other energy loss from reradiation of the reduction reactor ($Q_{re,radloss.reducer}$) cannot be neglected, which

accounts for 18.7% of the total solar energy input. The heat loss from oxidation reactor ($Q_{oxi,reactor}$) accounts for 3.6% of the total solar energy input. These three energy losses are the most significant in the cycle.

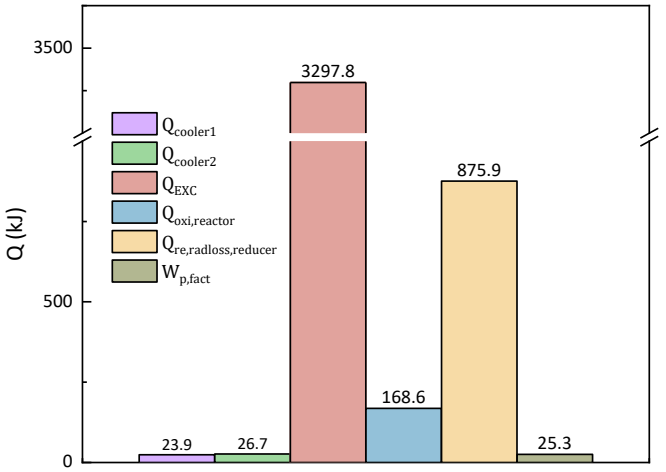

Fig. 3 Energy losses and power consumption distribution of solar thermochemical cycle

Fig. 4 shows the irreversibility distribution of the system. Among them, three types of irreversibility, denoted as IRR_{EXC}, $IRR_{re,reactor}$ and $IRR_{oxi,reactor}$, are the most significant, corresponding to the heat exchanger, the reduction reactor, and the oxidation reactor, which accounts for 72.2%, 23.7%, and 3.3%, respectively.

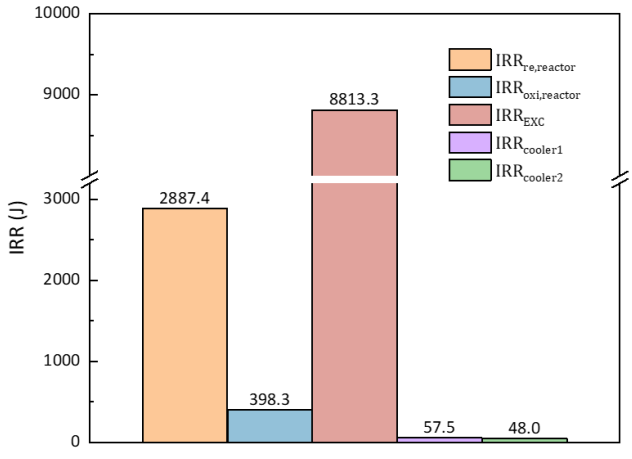

Fig. 4 Irreversibility distribution of solar thermochemical cycle

Fig. 5 illustrates the relationship of n_{CeO_2} vs T_H and n_{CeO_2} vs P. It can be observed that the increase of T_H leads to the decrease of n_{CeO_2}. This is due to the increase in temperature, which leads to an increase in the oxygen evolution of CeO_2 based on Le Chatelier's principle, consequently reducing n_{CeO_2} required to produce 1 mol of CO. As P increases, n_{CeO_2} also increases. This is due to the rise in pressure, which reduces the extent of the reduction reaction, and decreases the oxygen evolution of CeO_2, thereby increasing n_{CeO_2} needed to produce 1 mol of CO. Although there is no functional relationship between T_L and n_{CeO_2}, T_L is a critical characteristic variable within the system, and its relationship with other losses require further investigation. We will proceed with an analysis of the relationships between these irreversibility and these three characteristic variables (T_H, T_L, and P).

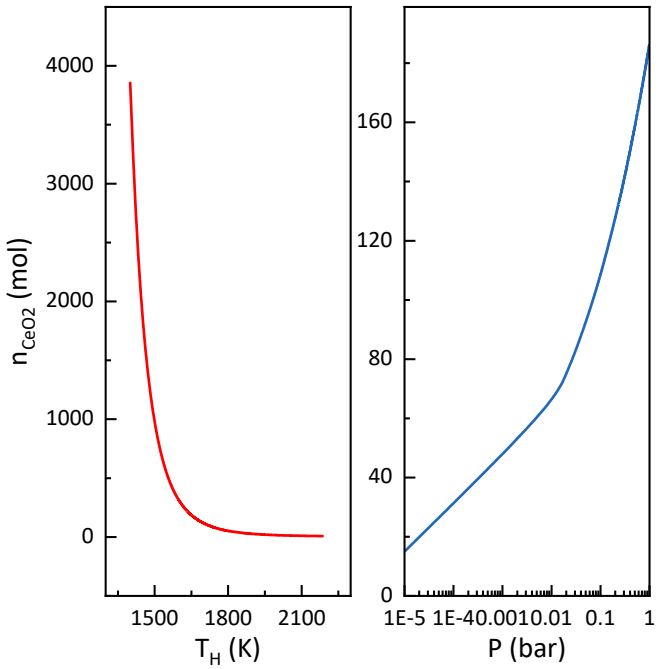

Fig. 5 The amount of CeO_2 versus reduction temperature(red) and pressure(blue)

3.2 Exergy analysis

The relationship between the temperature of the reduction reactor and irreversibility is shown in Fig. 6. With an increase in temperature, the irreversibility in the oxidation reactor remains nearly constant, while the irreversibility in the heat exchanger and the reduction reactor decreases. The irreversibility in the heat exchanger and the oxidation reactor exhibits a similar trend, ranging from 1700 K to 2100 K, whereas the irreversibility of the reduction reactor first decreases, and then increases, exceeding that of the heat exchanger at around 2100 K. This is because with the increase of T_H, n_{CeO_2} decrease, which leads to a decrease in Q_{EXC} because less CeO_2 is needed to produce 1 mol CO. This leads to a reduction in thermal entropy flow due to the heat transfer process. Additionally, the reduced amount of $CeO_{2-\delta}$ in the system results in a decrease in thermal entropy flow

due to the heating of reactants. Consequently, the irreversibility in the heat exchanger decreases. On the other hand, for the reduction reactor, the reduced temperature difference with the sun results in a decrease in thermal entropy flow due to the heat transfer process. However, a further increase in temperature after 2100 K enhances reradiation, leading to an increase in thermal entropy flow during the reradiation process. As a result, the irreversibility initially decreases, and then increases, ranging from 1700 K to 2200 K.

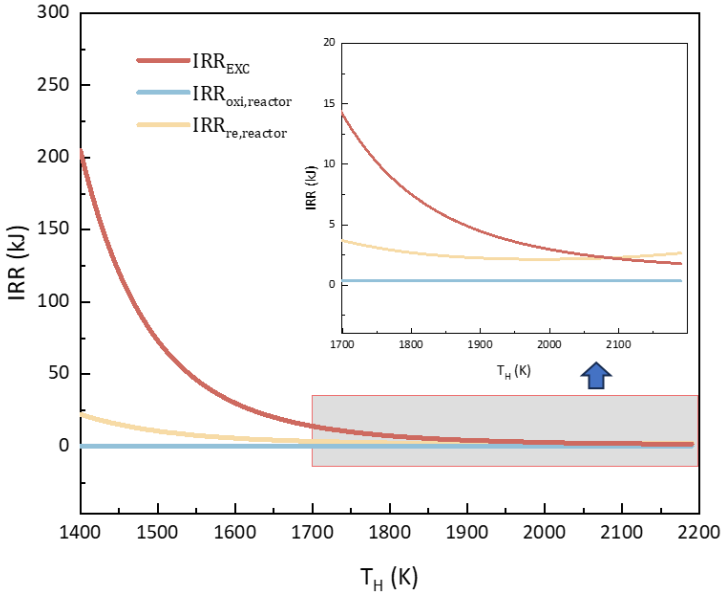

Fig. 6 Temperature versus irreversibility in a solar thermochemical cycle reduction reactor

The relation between oxygen partial pressure and irreversibility is illustrated in Fig. 7. With the increase in oxygen partial pressure, the irreversibility in the oxidation reactor remains nearly constant, while the irreversibility in the reduction reactor and the heat exchanger initially increases rapidly, and then increases more gradually. The reason for this is that the increased pressure leads to an increase in n_{CeO_2}, which leads to the increase in Q_{EXC} and the quantity of $CeO_{2-\delta}$ in the system because more CeO_2 is needed to produce 1 mol CO. This increases thermal entropy flow because of heat transfer processes and thermal entropy flow from heating of reactants in the heat exchanger, leading to an increase in the irreversibility of the heat exchanger. For the reduction reactor, an increase in n_{CeO_2} leads to an increase in reradiation losses and thermal entropy flow, because more heat is needed to reduce CeO_2, thus increasing the irreversibility of the reduction reactor.

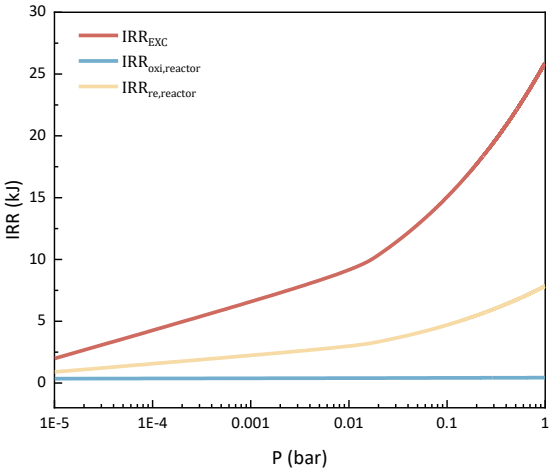

Fig. 7 Temperature at reduction reactor versus irreversibility for solar thermochemical cycle.

The relations between T_L and irreversibility is given in Fig. 8. With an increase in temperature, the irreversibility in the oxidation reactor remains nearly constant, while the irreversibility in the reduction reactor and the heat exchanger gradually decreases. The reason for this is that, as the temperature rises, there is a reduction in Q_{EXC} because of the decrease of temperature difference between T_L and T_H, leading to a decrease in thermal entropy flow generated by the heat transfer processes. Consequently, the irreversibility of the heat exchanger decreases. For the

reduction reactor, an increase in the exit temperature of CeO_2 from the oxidation reactor, which is due to the increased temperature, results in a decrease in $Q_{re,reactor}^{solar}$, and the thermal entropy flow generated by the heat transfer processes. This reduction leads to a decrease in the irreversibility of the reduction

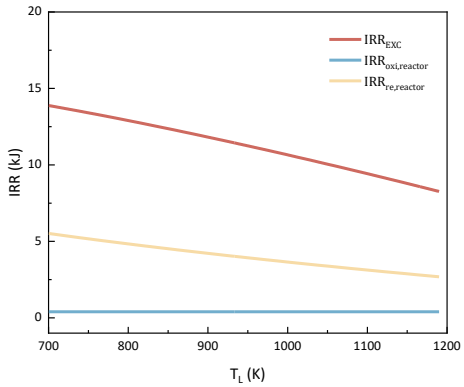

Fig. 8 Temperature at oxidation reactor vs irreversibility for solar thermochemical cycle.

Accoring to iterature[11], when δ>10^{-5} , the temperature range for T_H spans from 1400 K to 2000 K, T_L varies between 700 K and 1200 K, and P ranges from 10^{-5} to 1 bar. To comprehensively assess the distribution of irreversibility under various operating conditions, based on the permutation algorithm, we generated 300,000 combinations of T_H, T_L, and P, computed the irreversibility for each condition, subsequently arranged them in ascending order based on irreversibility magnitude. The results are shown in Fig. 9.

There are 11885 cases where the IRR is lower than the most efficient cases of the STF, known as “red case”. The lowest IRR case, known as “blue case”, is shown blue dot in Fig.9(b). The working condition and efficiency of blue and red dot are shown in Table 1.

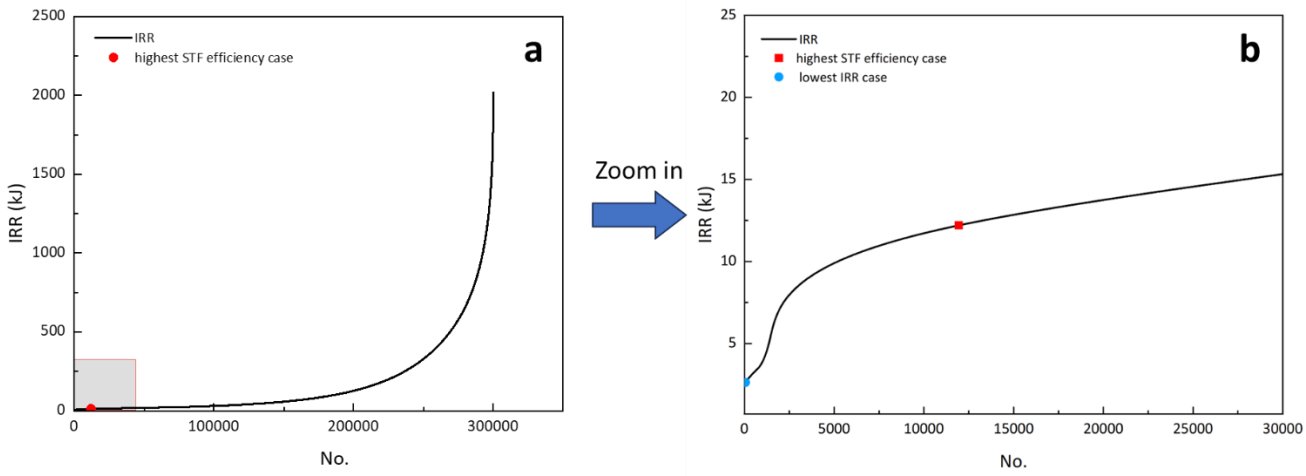

Fig. 9 (a) Irreversibility distribution at various operating points with increasing order of irreversibility magnitude. (b) Enlarged figure of the grey area in (a)

Table 1 Working condition and efficiency of highest STF case and lowest IRR case

	T_H	T_L	P	IRR	η_{STF}	η_{exergy}
Most efficient STF case	1773 K	1148 K	0.01 bar	12.20 kJ	5.25 %	6.55 %
Lowest IRR case	1960 K	1200 K	10^{-5} bar	2.52 kJ	12.65 %	12.51 %

The operating conditions with the lowest irreversibility are T_H and T_L values greater than the red case and pressure lower than the red case. The irreversibility in this blue case is reduced by 79% compared to the red case. In terms of efficiency, the solar-to-fuel efficiency for the blue case is 12.65%, and the exergy efficiency is 12.51%. Compared to the red case, there is a 141% improvement in energy efficiency and a 91% improvement in exergy efficiency.

4. CONCLUSIONS

This study establishes a thermodynamic model for Ce-based solar thermochemical cycles, analyzes the primary energy and exergy loss, elucidates the reasons

for the generation and variations of losses, and finds the working condition with the lowest irreversibility.

The overall analysis results indicate that the main energy losses and irreversibility are concentrated in the reduction reactor, heat exchanger, and oxidation reactor. These losses are corelated with n_{CeO_2}. As T_H increases, n_{CeO_2} decreases, and as P increases, n_{CeO_2} increases.

The exergy analysis results indicate that with an increase in T_H and T_L and a decrease in P, all three units reduce the irreversibility. This trend aligns with the findings from n_{CeO_2}. Moreover, the heoretical lowest irreversibility case is found, with 12.65% in energy efficiency and 12.51% in exergy efficiency while T_H= 1960 K, T_L= 1200 K and P = 10^{-5} bar. This provides suggestions for subsequent experiments.

ACKNOWLEDGMENT

The authors appreciate the support from the National Natural Science Foundation of China (No. 52090061 and No. 52225601).

DECLARATION OF INTEREST STATEMENT

The authors declare that they have no known competing financial interests or personal relationships that could have appeared to influence the work reported in this paper. All authors read and approved the final manuscript.

REFERENCE

[1] Ivanova M, Peters R, Müller M, et al. Technological Pathways to Produce Compressed and Highly Pure Hydrogen from Solar Power. Angew Chem Int Ed. Published online January 13, 2023:anie.202218850. doi:10.1002/anie.202218850

[2] Chen C, Jiao F, Lu B, Liu T, Liu Q, Jin H. Challenges and perspectives for solar fuel production from water/carbon dioxide with thermochemical cycles. Carbon Neutrality. 2023;2(1):9. doi:10.1007/s43979-023-00048-6

[3] Lewis NS, Nocera DG. Powering the planet: Chemical challenges in solar energy utilization. Proc Natl Acad Sci. 2006;103(43):15729-15735.

[4] Abanades S, Flamant G. Thermochemical hydrogen production from a two-step solar-driven water-splitting cycle based on cerium oxides. Sol Energy. 2006;80(12):1611-1623. doi:10.1016/j.solener.2005.12.005

[5] Chueh WC, Haile SM. A thermochemical study of ceria: exploiting an old material for new modes of energy conversion and CO 2 mitigation. Philos Trans R Soc Math Phys Eng Sci. 2010;368(1923):3269-3294. doi:10.1098/rsta.2010.0114

[6] Zhu L, Lu Y. Reactivity and Efficiency of Ceria-Based Oxides for Solar CO 2 Splitting via Isothermal and Near-Isothermal Cycles. Energy Fuels. 2018;32(1):736-746. doi:10.1021/acs.energyfuels.7b03284

[7] Marxer D, Furler P, Takacs M, Steinfeld A. Solar thermochemical splitting of CO 2 into separate streams of CO and O 2 with high selectivity, stability, conversion, and efficiency. Energy Environ Sci. 2017;10(5):1142-1149. doi:10.1039/C6EE03776C

[8] Bulfin B, Hoffmann L, De Oliveira L, et al. Statistical thermodynamics of non-stoichiometric ceria and ceria zirconia solid solutions. Phys Chem Chem Phys. 2016;18(33):23147-23154. doi:10.1039/C6CP03158G

[9] Brendelberger S, Von Storch H, Bulfin B, Sattler C. Vacuum pumping options for application in solar thermochemical redox cycles – Assessment of mechanical-, jet- and thermochemical pumping systems. Sol Energy. 2017;141:91-102. doi:10.1016/j.solener.2016.11.023

[10] Jiao F, Lu B, Chen C, Liu Q. Exergy transfer and degeneration in thermochemical cycle reactions for hydrogen production: Novel exergy-and energy level-based methods. Energy. 2021;219:119531.

[11] Panlener RJ. A THERMODYNAMIC STUDY OF NONSTOICHIOMETRIC CERIUM DIOXIDE. J Phys Chem Solids. 1975;11(36):1213-1222.